Biomaterials 32 (2011) 9434–9443

Contents lists available at SciVerse ScienceDirect

Biomaterials

journal homepage: www.elsevier.com/locate/biomaterials

The comparative effects of mesoporous silica nanoparticles and colloidal silica on inflammation and apoptosis

Soyoung Lee [a], Hui-Suk Yun [b,**], Sang-Hyun Kim [a,*]

[a] Laboratory of Immunotoxicology, Department of Pharmacology, School of Medicine, Kyungpook National University, 101 Dong-In, Jung-Gu, Daegu 700-422, Republic of Korea
[b] Engineering Ceramics Research Group, Functional Materials Division, Korea Institute of Materials Science (KIMS), 66 Sangnam, Changwon 641-831, Republic of Korea

ARTICLE INFO

Article history:
Received 21 June 2011
Accepted 16 August 2011
Available online 1 September 2011

Keywords:
Mesoporous silica nanoparticles
Colloidal silica nanoparticles
Apoptosis
Inflammation

ABSTRACT

Mesoporous silica (MPS), synthesized via the supramolecular polymer templating method, is one of the most attractive nanomaterials for biomedical applications, such as drug delivery systems, labeling, and tissue engineering. The significant difference between MPS and general silica (colloidal silica) is the pore architectures, such as specific surface area and pore volume. The pore structures of nanomaterials have been considered to be one of the key conditions, causing nanotoxicity due to their different efficiency of cellular uptake and immune response. We first studied the influence of pore structural conditions of silica nanoparticles on both inflammation and apoptosis, *in vitro* and *in vivo*, by comparing MPS and colloidal silica, and defined underlying mechanisms of action. Both the MPS and colloidal silica nanoparticles are produced by almost similar synthetic conditions, except the use of polymer template for MPS. The specific surface area of colloidal silica and MPS was 40 and 1150 $m^2\ g^{-1}$, respectively, while other conditions, including particle size (100 nm) and shape (spherical), were kept constant. In both MTT assay and FACS analysis, MPS nanoparticles showed significantly less cytotoxicity and apoptotic cell death than colloidal silica nanoparticles. MPS nanoparticles induced lower expression of pro-inflammatory cytokines, such as tumor necrosis factor-α, interleukin (IL)-1β, and IL-6, in macrophages. The reduced inflammatory response and apoptosis elicited by MPS nanoparticles were resulting from the reduction of mitogen-activated protein kinases, nuclear factor-κB, and caspase 3. In addition, using the local lymph node assay, a standalone *in vivo* method for hazard identification of contact hypersensitivity, we showed that colloidal silica nanoparticles act as an immunogenic sensitizer and induce contact hypersensitivity but not MPS nanoparticles. In conclusion, the pore architecture of silica nanoparticles greatly influences their biocompatibility and should be carefully designed. The MPS nanoparticles exhibit better biocompatibility than colloidal silica and promise excellent potential usage in the field of biomedical and biotechnological applications.

1. Introduction

With the growing progress of nanotechnology in biomedical applications, the use of nanomaterials as biomaterials has received considerable attention in both fundamental and technological developments [1,2]. Meanwhile, the unique physicochemical characteristics of nanomaterials raised concerns about their potential environmental and health impacts [3]. Current *in vitro* studies showed different ways in which nanomaterials could influence biological functions or induce cytotoxicity [4,5]. Because the physicochemical properties of nanoparticles are different from those of their bulk counterparts, their interaction with biological systems is expected to be different. Specifically, following accidental or intentional exposure, nanomaterials may stimulate and/or suppress the immune responses [6]. The use of nanomaterials in biomedical fields is likely to result in interactions between these materials and immune-competent cells, which are desirable for some applications, but may also trigger unwanted effects [7].

Many immunotoxic effects were shown to be due to interference with components of the signaling pathways involved in activation of the immune response, in particular with the mitogen-activated protein kinases (MAPKs) [8]. MAPKs are a group of oxidant-dependent signaling molecules potentially important in nanomaterial-induced inflammation and proliferative responses [9]. The MAPK signaling pathway has been shown to play a role in nuclear factor (NF)-κB activation through serine phosphorylation of IκB-α, leading to degradation of IκB-α [10]. NF-κB controls a variety of genes involved in immune, inflammatory, and proliferative

* Corresponding author. Fax: +82 53 423 4838.
** Corresponding author. Fax: +82 55 280 3392.
E-mail addresses: yuni@kims.re.kr (H.-S. Yun), shkim72@knu.ac.kr (S.-H. Kim).

0142-9612/$ – see front matter © 2011 Elsevier Ltd. All rights reserved.
doi:10.1016/j.biomaterials.2011.08.042

responses; these include various pro-inflammatory cytokines, such as tumor necrosis factor (TNF)-α, interleukin (IL)-1β and IL-6, and cell-adhesion molecules [11].

The effects of nanomaterials on cells may vary with different conditions of nanomaterials, depending on their chemical composition, crystallinity, size, shape and surface area [12]. Mesoporous silica (MPS), synthesized via the supramolecular polymer templating method, is one of the important members of nanomaterials in biomedical fields. MPS are a special class of synthetically modified colloidal silica, in which highly ordered pores in the meso-scale (2–50 nm) are introduced. MPS have received enormous attention in various biomedical applications, such as drug-/protein-/gene-delivery, labeling, bioseparation, transfection device, and tissue engineering, because of their unique pore architecture, that is, large specific surface area, pore volume, and controllable pore size [13–15]. Silica is generally considered to be non-cytotoxic [12]. However, development of MPS nanoparticles for biomedical use requires close attention to safety issues, because extremely high surface area of MPS could exert different effects on human health and environment. Previous studies concerning biocompatibility of MPS investigated the general conditions of nanomaterials, such as size, surface charge, and morphology [16–20]. The surface area of nanomaterials may also greatly affect on biocompatibility due to high reactivity. However, in spite of the extraordinary high surface area of MPS nanoparticles, no information regarding the effect of surface area on biocompatibility has been discussed. In this study, we first examined the effect of MPS nanoparticles on the cytotoxicity and the relationship between pore structural properties (surface area) and the biological response, as compared with colloidal silica nanoparticles in macrophages.

2. Materials and methods

2.1. Materials

Cetyltrimethyl-ammonium bromide (CTAB), tetraethyl orthosilicate (TEOS), ammonium hydroxide, HCl, ethanol, and methanol were purchased from Sigma–Aldrich (St. Louis, MO), and were used without further purification. Fluorescent probes, propidium iodide (PI) and Annexin V, were procured from Molecular Probes (Eugene, OR). PD98059, SB203580, SP600125, and pyrrolidine dithiocarbamate (PDTC) were purchased from Calbiochem (La Jolla, CA).

2.2. Nanoparticle preparation

MPS and colloidal silica nanoparticles were prepared using a similar process, except for the addition of the ionic surfactant CTAB, as a template to MPS. The MPS nanoparticles were prepared under dilute TEOS and low surfactant concentration condition, as follows: 0.66 g of CTAB was dissolved in a mixture of 800 ml of distilled water and 26.4 ml of ammonium hydroxide (29 wt% NH_3 in water); 3 ml of TEOS were then carefully added, with vigorous stirring. The precursor solution was stirred for another 3 h, at room temperature. To remove the surfactant template, the synthesized MPS was refluxed in a solution of 1 ml of HCl (37.4%) and 100 ml of methanol, followed by washing with methanol and water, repeatedly (10 times, in general). The surfactant-removed MPS were placed in ethanol and sonicated before using, to prevent aggregation of nanoparticles. The colloidal silica nanoparticles were synthesized in a similar process to MPS by mixing 500 ml of ethanol, 20 ml of distilled water, 20 ml of ammonium hydroxide, and 30 ml of TEOS. The precursor solution was then stirred for 24 h and filtered, washed with water, and re-dispersed in ethanol.

2.3. Structural characterizations

The structural characterization was carried out by field emission scanning electron microscopy (FE-SEM; JEOL5800, 5 kV) and transmission electron microscopy (TEM; JEOL-JEM2100F, 200 kV). The specific surface area and pore volume were measured by the N_2-gas adsorption method, using a BET apparatus (BEL Japan-Belsorp mini II).

2.4. Animals

Female BALB/c mice (8 weeks old) were purchased from Dae-Han Experimental Animal Center (Daejeon, Korea). The animals were housed in a laminar air flow room maintained under a temperature of 22 ± 2 °C and relative humidity of 55 ± 5% throughout the study. The care and treatment of the animal were in accordance with the guidelines established by the Public Health Service Policy on the Humane Care and Use of Laboratory Animals and were approved by the Institutional Animal Care and Use Committee.

2.5. Cell culture and viability

The BALB/c macrophage cell line J774A.1 (TIB-67, ATCC, Manassas, VA), was cultivated in Dulbecco's minimum essential medium and supplemented with 2 mM glutamine, 100 units/ml penicillin, 100 μg/ml streptomycin (1% antibiotics), and 10% non-heat-inactivated fetal bovine serum (Gibco, Grand Island, NY), under standard cell culture conditions (5% CO_2 at 37 °C). Three days after intraperitoneal injection of 2.5 ml of thioglycollate (TG) to 8 weeks old BALB/c mice, TG-elicited macrophages were harvested and isolated, as previously reported in Ref. [21]. Peritoneal lavage was performed using 8 ml of HBSS, which contained heparin. Then, cells were distributed in the culture media. Upon reaching confluence, cells were re-suspended, seeded at a density of 2×10^4 cells/well in 96-well plates, and treated with various concentrations of nanoparticles for either 1 day or 3 days. Cell viability was determined using the 3(4,5-dimethylthiazolyl-2)2,5-diphenyl tetrazolium bromide assay (MTT, Sigma). Specifically, MTT (10 mg/ml) was added into each well that contained a sample and incubated for 4 h. Isopropanol (in 0.04 N-HCl) was added to dissolve the formazan crystals. Absorbance was read at 570 nm using a spectrophotometer. Cell viability, defined as the relative absorbance on each sample compared to that of the control, was calculated and expressed as percentage.

2.6. Determining apoptosis and necrosis

To determine the presence of apoptosis and necrosis, cell death was analyzed by Annexin V and PI staining. For staining, cells (2×10^5 cells/well in 12-well plates) were treated with nanoparticles for 24 h. Cells were washed with PBS, centrifuged, and suspended in Annexin V binding buffer containing 5 μl/100 μl of Annexin V and PI (final concentration 5 μg/ml). Cells were incubated for 15 min at 37 °C and analyzed using the flow cytometer (BD Biosciences, San Diego, CA). The Fluorochrome was excited using the 488 nm line of argon ion laser, and Annexin V and PI emissions were monitored at 525 and 620 nm, respectively. A total of at least 1×10^4 cells were analyzed per sample.

2.7. Polymerase chain reaction (PCR)

Reverse transcription-polymerase chain reaction (RT-PCR) was used to analyze the expression of mRNA for various cytokines. The total cellular RNA was isolated from cells (2×10^5 cells/ml in 24-well plate), using the protocol described earlier in Ref. [22]. First strand complimentary DNA (cDNA) was synthesized from 2 μg of total RNA, using a Maxime RT-PreMix Kit (iNtRON Biotechnology, Daejeon, Korea). The respective primers were chosen by the Primer3 program (Whitehead Institute, Cambridge, MA) and all primers were obtained from Genotech (Daejeon, Korea). PCR was carried out with the following primers: TNF-α (F 5′-GGC AGG TCT ACT TTG GAG TCA TTG C-3′; R 5′-ACA TTC GAG GCT CCA GTG AAT TCG G-3′), IL-1β (F 5′-ATA ACC TGC TGG TGT GTG AC-3′; R 5′-AGG TGC TGA TGT ACC AGT TG-3′), IL-6 (F 5′-CCG GAG AGG AGA CTT CAC AG-3′; R 5′-GGA AAT TGG GGT AGG AAG GA-3′). β-actin (F 5′-TAG ACT TCG AGC AGG AGA TG-3′; R 5′-TTG ATC TTC ATG GTG CTA GG-3′) was used to verify the equal amounts of cDNA. The annealing temperature and cycles were 55 °C, 30 cycles for TNF-α, 55 °C, 30 cycles for IL-1β, 60 °C, 35 cycles for IL-6, and 55 °C, 30 cycles for β-actin. Products were separated by electrophoresis on a 1.5% agarose gel and visualized by staining with ethidium bromide. The gels were certificated using a Kodak DC 290 digital camera.

Quantitative real-time PCR was also carried out to verify mRNA expression, using the Thermal Cycler Dice Real Time System (TP-800; TakaRa Bio Inc.). Briefly, 2 μl of cDNA (100 ng), 1 μl each of sense and antisense primer solution (0.4 μM), 12.5 μl of SYBR Premix Ex Taq, and 9.5 μl of dH_2O were mixed together to obtain a final 25 μl reaction mixture in each reaction tube. The amplification conditions were 10 s at 95 °C, 40 cycles of 5 s at 95 °C and 30 s at 60 °C, 15 s at 95 °C, 30 s at 60 °C, and 15 s at 95 °C. Relative quantification of mRNA expression was performed using the TP850 software. Lipopolysaccharide (LPS) was used as a positive control.

2.8. Nuclear protein extraction

Preparation of the nuclear extract was described elsewhere [23]. Briefly, after cell activation with nanoparticles for the indicated times, cells (2×10^6 cells/well in 6-well plates) were washed in 1 ml of ice-cold PBS, re-suspended in 100 μl of ice-cold hypotonic buffer (10 mM HEPES/KOH, 2 mM $MgCl_2$, 0.1 mM EDTA, 10 mM KCl, 1 mM DTT, 0.5 mM PMSF, pH 7.9), left on ice for 10 min, vortexed, and centrifuged at 15,000 *g* for 30 s. Pelleted nuclei were gently re-suspended in 20 μl of ice-cold saline buffer (50 mM HEPES/KOH, 50 mM KCl, 300 mM NaCl, 0.1 mM EDTA, 10% glycerol, 1 mM DTT, 0.5 mM PMSF, pH 7.9), left on ice for 20 min, vortexed, and centrifuged at 15,000 *g* for 5 min at 4 °C. Aliquots of the supernatant that contained nuclear proteins were frozen in liquid nitrogen and stored at −70 °C.

2.9. Western blot

Samples for Western blot were prepared as previously described [24]. Cells (2×10^6 cells/well in 6-well plates) were incubated for the indicated times: 30 min for MAPKs, 2 h for NF-κB, 24 h for caspase 3. In brief, cells were then rinsed twice with ice-cold PBS, and total cell lysates were gathered in 200 μl of lysis buffer (20 mM Tris–HCl, 120 mM NaCl, 50 mM HEPES, 1% Triton-X, 1 mM EDTA, 2 mM sodium orthovanadate, 1 mM DTT, 10% glycerol, 0.02 mM PMSF, 1 mg/ml leupeptin, 1 mg/ml aprotinin). The lysates were spun in a micro-centrifuge for 20 min at 4 °C, and the supernatant was collected. Proteins were electrophoresed using 8–12% SDS-PAGE, and then transferred to nitrocellulose membranes. The membranes were stained with reversible Ponceau S to ascertain equal loading of samples in the gel. The caspase 3, p65 NF-κB, and IκB-α were assayed using anti-pro-caspase 3, anti-NF-κB (p65) and anti-IκB-α antibodies (Santa Cruz Biotech, Santa Cruz, CA). The p38, JNK, and ERK activation was determined using anti-phospho-p38, -JNK, and -ERK antibodies (Cell Signaling, Beverly, MA). Immunodetection was performed using an enhanced chemiluminescence detection kit (Amersham, Piscataway, NJ).

2.10. Local lymph node assay (LLNA)

The murine LLNA is recognized by the United States Interagency coordinating Committee on the Validation of Alternative Methods (ICCVAM) as a standalone method for hazard identification of contact hypersensitivity [25]. Female BALB/c mice (8 weeks old) were allocated randomly to dose and control groups for each sample ($n = 5$ per group). A 25 μl aliquot of test solution or solvent only (4:1, acetone:olive oil, AOO) was applied daily to the dorsum of both ears of each mouse, for three consecutive days (days 1–3). The positive controls for this study received 0.15% 2,4-dinitroflourobenzene (DNFB). For the co-treatment of DNFB and nanoparticles, nanoparticles were treated 2 h before the DNFB treatment. Measurements of ear thickness were performed using a dial thickness gauge on days 1–3. The mice were rested on days 4 and 5. On day 4, 24 h after the last treatment, measurements of ear thickness were made to assess treatment-induced irritancy. For the LLNA, 20 μCi ^{3}H-thymidine in 250 μl PBS was injected via the tail vein into all test and control mice, on day 6. After 5 h, the auricular lymph nodes were excised. Single-cell suspensions of lymph node in 5 ml of PBS were prepared by passage through sterile 100 μm nylon cell strainers (Falcon, Bedford, MA). The lymph node cell suspension was washed twice with an excess of PBS, and the cell pellet was incubated in 3 ml of 5% trichloroacetic acid at 4 °C for approximately 18 h. Each cell pellet was re-suspended in 1 ml of trichloroacetic acid and transferred to 9 ml of scintillation fluid. The counts per min (cpm) were measured with liquid scintillation spectrophotometry.

2.11. Statistical analysis

Statistical analyses were performed using the SAS statistical software (SAS Institute, Cary, NC). Treatment effects were analyzed using one-way ANOVA, followed by Duncan's multiple range tests. Statistical significance was set at $P < 0.05$.

3. Results

3.1. Characterization of materials

FE-SEM images of colloidal silica (Fig. 1A) and MPS (Fig. 1B) indicate that both nanoparticles showed same morphology (as spherical), with diameters in about 100 nm, and were well discrete.

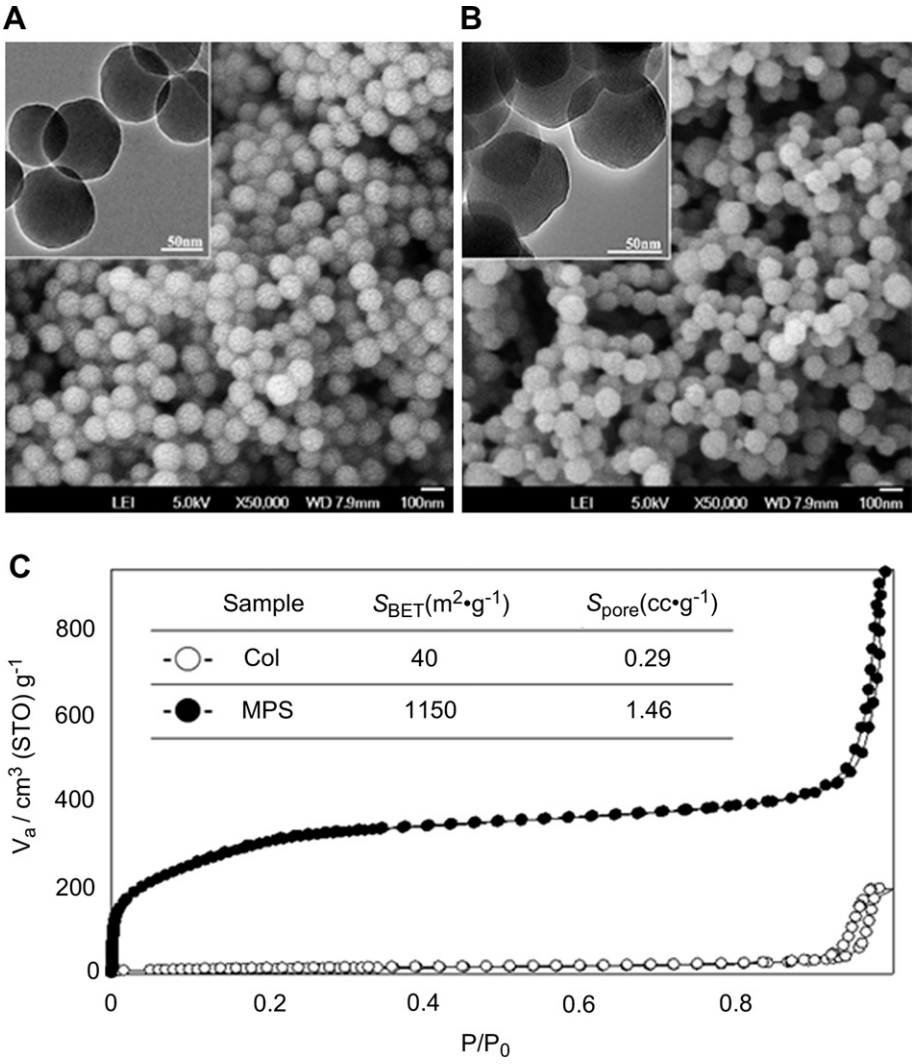

Fig. 1. FE-SEM images and TEM images (inset) of (A) colloidal silica, (B) MPS and (C) N_2 adsorption–desorption isotherms of colloidal silica and MPS nanoparticles.

A hexagonally well-ordered mesostructure, with the average pore size of 2.4 nm, were observed by TEM observation in MPS (Fig. 1B inset), while no pore structure was observed in colloidal silica (Fig. 1A inset and SI. 1). CTAB used as polymer template was well removed by solvent extraction process (SI. 2). MPS had a BET specific surface area of 1150 $m^2\ g^{-1}$ and pore volume of 1.46 $cm^3\ g^{-1}$, while the corresponding value of colloidal silica were 40 $m^2\ g^{-1}$ and 0.29 $cm^3\ g^{-1}$, respectively (Fig. 1C).

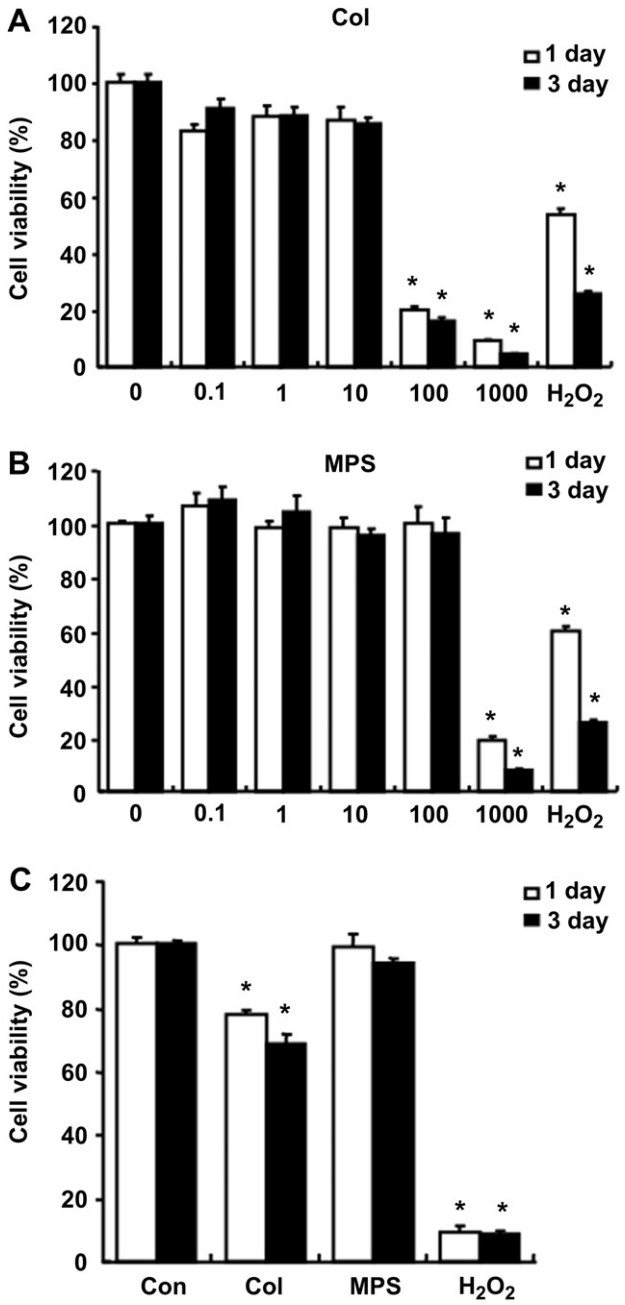

Fig. 2. Effects of nanomaterials on cell viability in macrophages. J774A.1 macrophages (2×10^4 cells/well in 96-well plates) were treated with various concentrations of (A) colloidal silica nanoparticles and (B) MPS nanoparticles, for 1 day or 3 days. (C) Primary cultured peritoneal macrophages were treated with 100 μg/ml of colloidal silica nanoparticles and MPS nanoparticles for 1 day or 3 days. The cell viability was determined using the MTT assay. Hydrogen peroxide (500 μM) was used as the positive control. Cell viability was determined by the relative absorbance, compared to control. The results were presented as mean ± SEM of three independent experiments. *Significantly different from the control. Col: colloidal silica nanoparticles. MPS: mesoporous silica nanoparticles.

3.2. Cell viability

We examined whether MPS and colloidal silica nanoparticles possess cytotoxicity. J774A.1 macrophage cells were exposed to various amounts of MPS and colloidal silica nanoparticles for 1 or 3 days. The colloidal silica nanoparticles were highly toxic to macrophages at 100 μg/ml. However, MPS nanoparticles up to 100 μg/ml did not affect cell viability, while the colloidal silica nanoparticles killed 80.25% of cells (Fig. 2A and B). Similarly, using the primary cultured peritoneal macrophages, we found that colloidal silica nanoparticles were more toxic than MPS nanoparticles (Fig. 2C). Hydrogen peroxide was used as a positive control.

To confirm the difference in toxicity between colloidal silica and MPS nanoparticles, we examined apoptotic cell death, using flow cytometry. Cells were treated with MPS or colloidal silica nanoparticles at 100 μg/ml concentration for 24 h. The normal cells were stained with only a low level of fluorescence; however, apoptotic cells were stained with a higher fluorescence by Annexin V staining. Colloidal silica nanoparticles induced apoptotic cell death based on high fluorescence by Annexin V (Fig. 3A). This data mean that colloidal silica nanoparticles induced cytotoxicity by apoptosis. Comparing with colloidal silica nanoparticles, MPS nanoparticles did not cause apoptotic cell death. To further evaluate apoptotic signaling by nanoparticles, the activation of caspase 3 was measured. Caspase 3 belongs to the cysteine protease family and is responsible for cleaving substrates, such as the DNA fragmentation factor that can go on to damage DNA, and is thus considered to be the effector caspase. Our data showed that caspase 3 was activated by silica nanoparticles; however, activation of caspase 3 was lower on MPS nanoparticles (Fig. 3B). These findings suggest that MPS

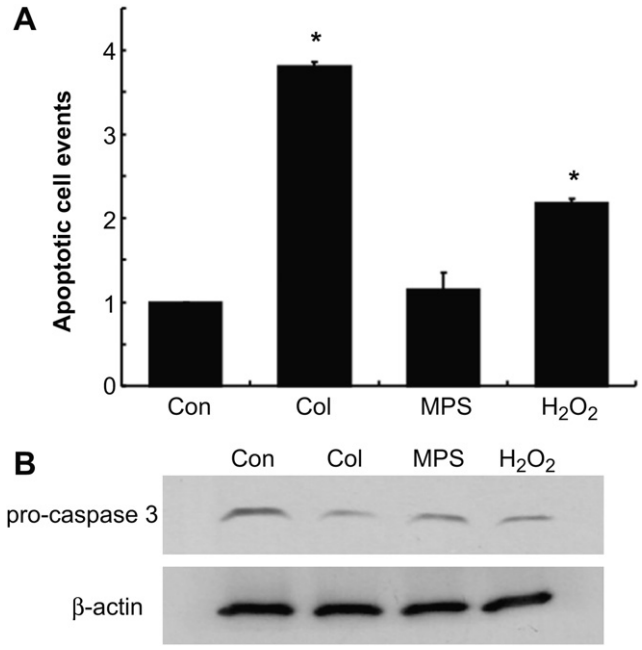

Fig. 3. Effect of nanomaterials on apoptosis and caspase 3 activation. (A) J774A.1 macrophages (2×10^5 cells/well in 12-well plates) were treated with 100 μg/ml of either colloidal silica nanoparticles or MPS nanoparticles for 24 h. Cells were stained with Annexin V and then analyzed using a flow cytometer. Hydrogen peroxide (500 μM) was used as a positive control. The results were presented as mean ± SEM of three independent experiments. *Significantly different from the control. (B) J774A.1 macrophages (2×10^6 cells/well in 6-well plates) were treated with 100 μg/ml of either colloidal silica nanoparticles or MPS nanoparticles for 24 h and the blots were examined with anti-caspase 3 antibody. Col: colloidal silica nanoparticles. MPS: mesoporous silica nanoparticles.

nanoparticles induced lower cytotoxicity in macrophages, compared with colloidal silica nanoparticles.

3.3. Expression of pro-inflammatory cytokines

Pro-inflammatory cytokines (e.g. TNF-α, IL-1β, and IL-6) released from macrophages play an important role in the inflammation process. To investigate the effect of nanoparticles on the pro-inflammatory cytokines, we treated cells with either colloidal silica nanoparticles or MPS nanoparticles, at 100 μg/ml for 6 h, and the gene expression of cytokines was measured by RT-PCR and quantitative real-time PCR. When the J774A.1 cells were treated with colloidal silica nanoparticles, the expression of all cytokines was increased (Fig. 4A and B). On the contrary, MPS nanoparticles showed less induction of cytokine expressions. Next, we confirmed the effect of nanoparticles on the cytokine expression using primary cultured peritoneal macrophages (Fig. 4C and D). As results, MPS nanoparticles induced much lower cytokine expression than colloidal silica nanoparticles. These results suggest that MPS nanoparticles mitigated the inflammatory response by down-regulating the pro-inflammatory cytokines.

3.4. Activation of MAPK and NF-κB

MAPKs and NF-κB are key intercellular mediators of inflammatory signaling and control the transcription of many signaling genes. To determine the effect of silica nanoparticles on MAPK activation, we studied the phosphorylation of three types of MAPKs: ERK, p38 and JNK (Fig. 5A). Colloidal silica nanoparticles induced higher activation of ERK, p38 and JNK than MPS nanoparticles.

Treatment with colloidal silica nanoparticles induced the degradation of IκB-α, and the nuclear translocation of p65 NF-κB, after 2 h of incubation (Fig. 5B). However, treatment with MPS nanoparticles induced much less degradation of IκB-α, and less nuclear translocation of NF-κB. These results indicate that colloidal silica nanoparticles induced inflammation through the activation of both MAPKs and NF-κB.

To confirm the role of MAPKs and NF-κB on the colloidal silica nanoparticles induced cytotoxicity, cells were treated with various pharmacological inhibitors for ERK (10 μM PD98059), p38 (2.5 μM SB203580), JNK (2.5 μM SP600125) and NF-κB (20 μM PDTC), 30 min prior to the treatment of colloidal silica nanoparticles. Following the exposure, the IL-1β expression and Annexin V staining was tested in macrophages (Fig. 6A and B). The results demonstrated that the IL-1β expression and apoptosis were significantly decreased when cells were pretreated with PD98059, SB203580, SP600125, and PDTC before colloidal silica nanoparticles. These inhibitors have protective effects on colloidal silica nanoparticles induced IL-1β expression and apoptosis. These data suggest that ERK, p38, JNK, and NF-κB play a role in colloidal silica nanoparticles induced inflammation and apoptosis.

3.5. Effect of nanoparticles on hypersensitivity and lymphocyte proliferation

We tested the effects of nanoparticles on the immune response induced by the contact dermatitis sensitizer DNFB (positive

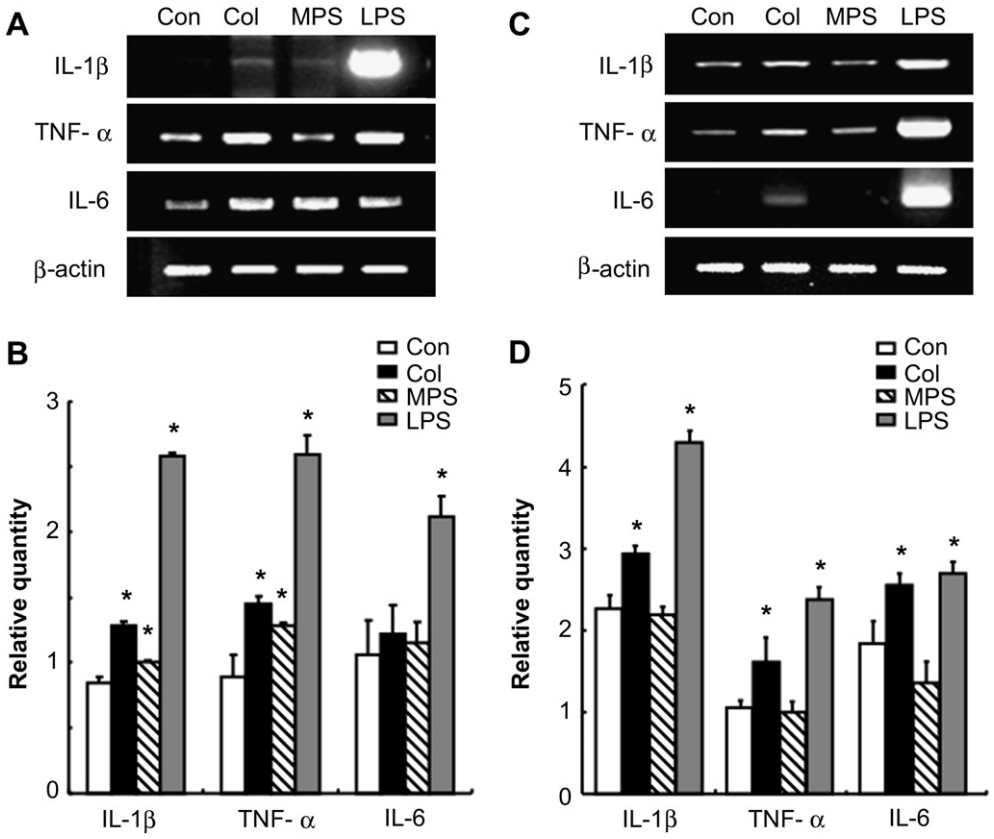

Fig. 4. Effects of nanomaterials on expression of pro-inflammatory cytokines. Cells (2×10^5 cells/well in 24-well plates) were treated with 100 μg/ml of either colloidal silica nanoparticles or MPS nanoparticles for 6 h. The total cellular RNA was isolated from the cell and the expression of mRNA for TNF-α, IL-1β, and IL-6 cytokines was analyzed by RT-PCR and real-time PCR in J774A.1 cells (A and B) or in primary peritoneal macrophages (C and D). LPS (lipopolysaccharide, 30 ng/ml) was used as a positive control. The results were presented as mean ± SEM of three independent experiments. *Significantly different from the control. Col: colloidal silica nanoparticles. MPS: mesoporous silica nanoparticles.

control), using an adapted local lymph node assay (LLNA). LLNA was developed as a predictive test method for the identification of chemicals that have the potential to induce contact hypersensitivity [26]. In the LLNA, lymphocyte proliferation in draining lymph nodes is used as a measure for the immune response to an applied allergen. As such, the LLNA can be seen as a functional assay of immune reactivity, which is suggested to be applicable in the study of direct effects on the immune system after exposure to materials. The effects of nanomaterials are shown in Fig. 7. In spite of no changes of body weight in all groups (Fig. 7A), significant changes have been seen in ear thickness (Fig. 7B). From day 2, DNFB induced increase of ear thickness. Colloidal silica nanoparticles alone also induced increase of ear thickness from day 2. Comparing with colloidal silica nanoparticles, MPS nanoparticles induced less increase of ear thickness. Interestingly, in a co-treatment with DNFB and nanoparticles, colloidal silica nanoparticles enhanced the DNFB-induced ear thickness at day 4 and day 6. These enhanced effects were reduced in co-treatment of DNFB and MPS nanoparticles. Next, we measured the lymphocyte proliferation in draining lymph nodes (Fig. 7C). As expected, DNFB induced lymphocyte proliferation. In a co-treatment with DNFB and nanoparticles, colloidal silica nanoparticles enhanced the DNFB-induced lymphocyte proliferation in the draining lymph nodes, but not MPS nanoparticles. These data suggest that colloidal silica nanoparticles evoked contact hypersensitivity. However, changes of pore structural properties to MPS nanoparticles, such as high specific surface area and pore volume, could reduce these adverse effects.

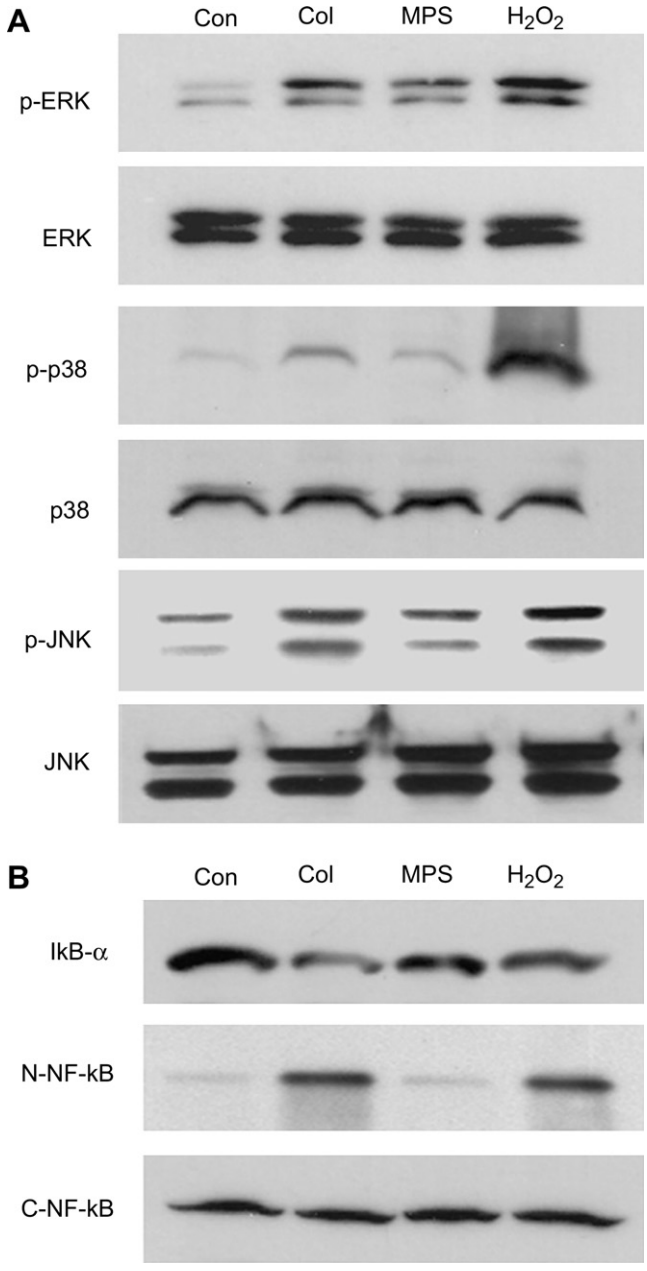

Fig. 5. Effects of nanomaterials on MAPKs and NF-κB activation. J774A.1 macrophages (2×10^6 cells/well in 6-well plates) were stimulated with 100 μg/ml of either colloidal silica nanoparticles or MPS nanoparticles at indicated times. (A) The phosphorylation of ERK, JNK and p38 was analyzed by Western blot. (B) The degradation of IκB-α and the nuclear translocation of NF-κB were analyzed by Western blot. Hydrogen peroxide (500 μM) was used as a positive control. Col: colloidal silica nanoparticles. MPS: mesoporous silica nanoparticles.

4. Discussion

MPS nanoparticles have been widely investigated in the field of drug delivery, drug targeting, tissue engineering, gene transfection

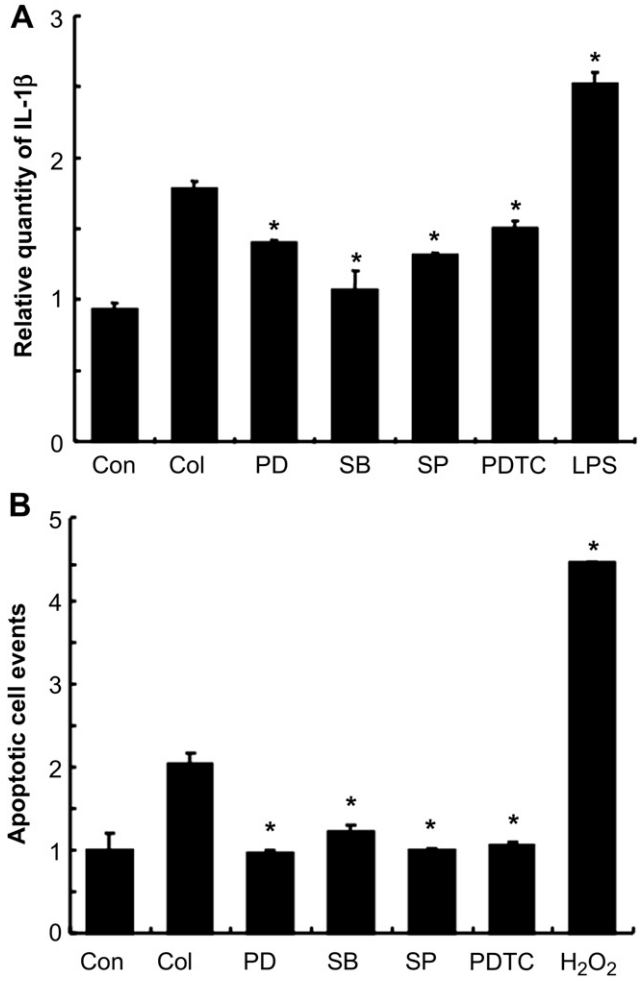

Fig. 6. Effects of specific inhibitors on nanomaterial-induced cytotoxicity. All pharmacological agents (i.e. PD 98059: 10 μM, SB 203580: 2.5 μM, SP 600125: 2.5 μM, PDTC: 20 μM) were added 30 min before the treatment of colloidal silica nanoparticles. (A) The total cellular RNA was isolated from the cells (2×10^5 cells/ml in 24-well plate) and the expression of mRNA for IL-1β was analyzed by RT-PCR. (B) Cells (2×10^5 cells/well in 12-well plates) were stained with Annexin V and then analyzed using the flow cytometer. Hydrogen peroxide (500 μM) and LPS (30 ng/ml) were used as the positive control. The results were presented as mean ± SEM of three independent experiments. *Significantly different from the colloidal silica nanoparticles. Col: colloidal silica nanoparticles.

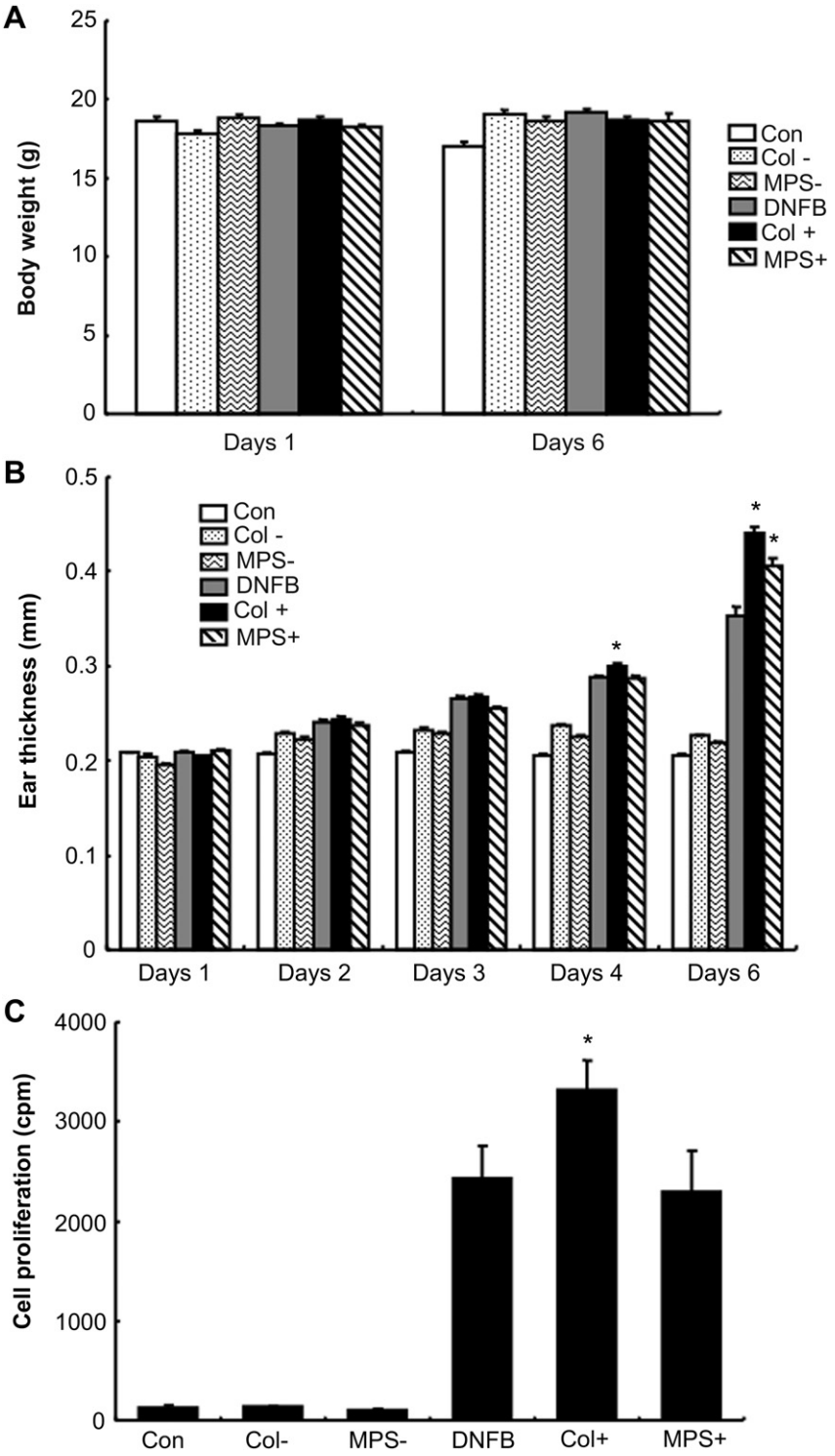

Fig. 7. Effects of nanomaterials on hypersensitivity and lymphocyte proliferation. BALB/c mice were treated with either the test-substance (1 mg/ear in alcohol) or vehicle (4:1 acetone:olive oil solution) to the dorsum of both ears on days 1–3, and were rested on days 4 and 5. DNFB (2,4-dinitroflourobenzene, 0.15%) was used as a positive control. Col+ and MPS+ represent co-treatment of DNFB and nanomaterials. (A) The body weight was measured on day 1 and day 6. (B) The ear thickness was measured with a dial thickness gauge. On day 4, i.e. 24 h after the last treatment, ear thickness was measured to assess treatment-induced irritancy. (C) For the LLNA, mice were injected intravenously with 20 μCi ^{3}H-thymidine in 250 μl PBS, on day 6. After 5 h, the lymph nodes were excised. Lymph node cells were lysed and incubated overnight in 5% trichloroacetic acid, and cpm were measured by liquid scintillation spectrophotometry. The results were presented as mean ± SEM of three independent experiments. *Significantly different from the DNFB value. Col−: colloidal silica nanoparticles without DNFB. MPS−: mesoporous silica nanoparticles without DNFB. Col+: colloidal silica nanoparticles with DNFB. MPS+: mesoporous silica nanoparticles with DNFB.

and cell tracking [12,17,27–30]. The unique mesoporous structure of these particles is the cause for the broad interest in their application in biotechnology. Their large internal volumes and high surface areas allow for high adsorption of drugs and proteins into their structures [31]. However, the biological response to these materials has been much less characterized. The distinct physicochemical properties of nanoparticles indeed determine their interaction with the cell/within the cell, and even subtle differences in such properties can modulate their toxicity and modes of action [32]. However, these cytotoxicity studies have focused mainly on the cellular functional assay, rather than highlighting the particularities of biomedical application of different nanoparticles. Although some studies have suggested that nanoparticles could be applied in biomedicine due to their biosafety, a standardization of cytotoxicity evaluation is still required before the material can be deemed non-cytotoxic [33].

The principal purpose of this research is to evaluate the toxicity of MPS nanoparticles comparing with colloidal silica nanoparticles. In a recent study, severe inflammation following exposure to silica particles appeared to be the common initiating step [34]. When tested on macrophages, vitreous silica and pure quartz showed a remarkable potency in cytotoxicity, release of nitrite and TNF-α, suggesting a common behavior in inducing oxidative stress [35]. Our results showed that exposure of macrophages to colloidal silica nanoparticles increased cytotoxicity at the concentration of 100 μg/ml; however, MPS nanoparticles showed significantly less cytotoxicity than colloidal silica nanoparticles in both time- and dose-dependent manner (Fig. 2A and B). Although we cannot assert toxicity of colloidal silica with this experiment because concentration of 100 μg/ml is extremely harsh condition to cells, we can determine that the increase of surface area of colloidal silica induce the decrease of toxic effect under same harsh condition. In addition, MPS nanoparticles showed significantly less induction of pro-inflammatory cytokines than colloidal silica nanoparticles (Fig. 4). These results suggest that MPS nanoparticles elicit less toxicity and inflammation than conventional colloidal silica nanoparticles.

Some studies identified oxidative stress-related changes in gene expression and cell signaling pathways as the main traits of nanoparticle-induced cytotoxicity [36]. In mammalian macrophages, components of kinase-mediated cell signaling, in particular the stress-activated p38 and JNK, play a key role in the activation of the immune response induced by bacterial challenge and inflammatory cytokines. The activation of the stress-activated MAPKs was associated to phosphatidyl serine externalization, indicating apoptotic processes, and to cell damage [37]. In addition, it was reported that silica activates p38 and JNK in Raw 264.7 macrophages. Their signaling pathways link to activation of NF-κB, leading to the induction of early response genes that are critical in inflammation [38]. In our result, colloidal silica nanoparticles strongly activated ERK, p38, and JNK, compared with MPS nanoparticles (Fig. 5A). In addition, the activation of NF-κB showed similar results, i.e. MPS nanoparticles less activated NF-κB than colloidal silica nanoparticles (Fig. 5B). These findings suggest that the less activation of MAPKs and NF-κB by MPS nanoparticles may be responsible for the decreased toxicity and pro-inflammatory cytokines expression. A possible pathway for the influence of silica nanoparticle on cell damage based on our study is summarized in Scheme 1.

During the development of biomaterials, *in vivo* studies are regarded as a critical check point. *In vitro* study could be easily interfered by cell types, expose time, and experiment conditions [39]. Therefore, *in vivo* study is needed when there is a risk for the possible differences in bioavailability which may cause therapeutic inequivalence. We confirmed our *in vitro* results using local lymph node assay (LLNA). LLNA has been shown to predict the toxicity of small molecule drugs toward the immune system and identifies chemical sensitizers by their capacity to induce significant draining lymph node cell proliferation following dermal exposure [25]. An immunosuppressive or immunostimulating effect of the test agents would be expressed by a cell proliferation and cytokine response of lymphocytes after application of the sensitizer [26]. In addition, LLNA is the *in vivo* test used to determine if a test-substance can induce delayed-type hypersensitivity (DTH). DTH can result in organ and tissue damage, and involves a complex set of reactions especially contact hypersensitivity [40]. In the present study, colloidal silica nanoparticles induced increase of ear thickness. More importantly, colloidal silica nanoparticles exacerbated DNFB-induced ear thickness and lymphocytes proliferation. These results suggest that colloidal silica nanoparticles act as an immunogenic sensitizer and induce contact hypersensitivity. These negative effects were suppressed by the change of pore architecture from non-porous to nanoporous, indicating better biocompatibility of MPS than those of colloidal silica through not only *in vitro* test but *in vivo* test.

The physicochemical properties of silica nanoparticles play a crucial role in determining their potential interactions with biological systems. Surface area, surface morphology, surface energy, dissolution layer properties, absorption and aggregation properties are all relevant parameters. Surface silanol groups are directly involved both in membranolysis and in cytotoxicity. Both distribution and abundance of silanols determines the degree of cytotoxicity [41,42]. The representative difference in physicochemical properties between MPS and colloidal silica nanoparticles is the porosity. That is, MPS are composed with much plentiful external silanol group due to large surface specific area than colloidal silica. By the different conditions of pore architecture, we found that MPS

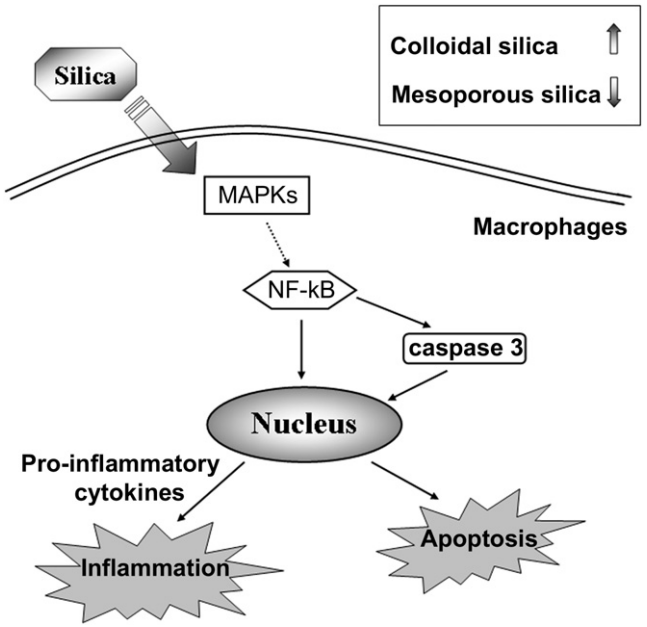

Scheme 1. A tentative schematic indicating the pathways involved in silica nanoparticles induced cell damage. Silica nanoparticles activate all three types of MAPKs and may stimulate downstream NF-κB. This may activate expression of pro-inflammatory cytokines and caspase 3. NF-κB-mediated expression of pro-inflammatory cytokines and activation of caspase 3 are the signaling for silica-induced inflammatory reaction and apoptosis, respectively; because specific inhibitors for the MAPKs and NF-κB prevented silica-induced expression of pro-inflammatory cytokines and apoptosis. Only pathways relevant to present discussion are illustrated; other signaling for both inflammation and apoptosis may also be involved.

nanoparticles elicit decreased cytotoxicity and inflammatory response in macrophages. Similarly, a recent study indicated that silica particles with extremely high surface area do not impair the essential functional responses of human macrophages, such as engulfment of the target cells and cytokine secretion [20]. Studies on interaction of MPS particles indicate that these mesoporous materials exert low toxicity in primary human dendritic cells [43]. The uptake of MPS did not decrease the ability of macrophages to ingest apoptotic or antibody opsonized target cells. These findings thus point to a low degree of cytotoxicity of MPS [20]. Similarly, no cytotoxicity of the MPS was observed in a number of cancer cell lines or in the macrophage cell line, RAW 264.7 [29]. In contrast, the cytotoxicity of colloidal silica nanoparticles in cultured human alveolar epithelia cells and hepatic cells increased in a time- and dose-dependent manner [44,45].

5. Conclusions

We demonstrated the effect of pore structural conditions of silica nanoparticles on inflammation and apoptosis, and defined underlying mechanisms of action. Mesoporous silica nanoparticle, MPS, with high porosity induced the reduction of *in vitro* cytotoxicity and inflammation compared with non-porous silica nanoparticle, colloidal silica. The less activation of MAPKs, NF-κB, and caspase 3 by MPS is apparently responsible for the decrease of toxicity and expression of pro-inflammatory cytokines. The results of *in vivo* test for hazard identification of contact hypersensitivity also revealed same phenomena to *in vitro*. The characteristics of pore structure of silica nanoparticles were strongly related with their biocompatibility and therefore should be carefully controlled for use in biomedical applications. Within the limits of the present study, it can be concluded that MPS exhibit favorable biocompatibility both *in vitro* and *in vivo*, and could play a key role in various intracellular processes for many future biomedical applications.

Acknowledgments

This work was supported by the Mid-career Researcher Program through an NRF grant funded by the MEST (No. 2010-0027969 and No. 2011-0017572) and by the Grant of the Korean Ministry of Education, Science and Technology (The Regional Core Research Program/Anti-aging and Well-being Research Center).

Appendix. Supplementary material

Supplementary data associated with this article can be found, in the online version, at doi:10.1016/j.biomaterials.2011.08.042.

References

[1] Sahoo SK, Labhasetwar V. Nanotech approaches to drug delivery and imaging. Drug Discov Today 2003;8:1112–20.
[2] Wilkinson JM. Nanotechnology applications in medicine. Med Device Technol 2003;14:29–31.
[3] Colvin VL. The potential environmental impact of engineered nanomaterials. Nat Biotechnol 2003;21:1166–70.
[4] Yin H, Too HP, Chow GM. The effects of particle size and surface coating on the cytotoxicity of nickel ferrite. Biomaterials 2005;26:5818–26.
[5] Gupta AK, Gupta M. Cytotoxicity suppression and cellular uptake enhancement of surface modified magnetic nanoparticles. Biomaterials 2005;26:1565–73.
[6] Dobrovolskaia MA, McNeil SE. Immunological properties of engineered nanomaterials. Nat Nanotechnol 2007;2:469–78.
[7] Slowing II , Vivero-Escoto JL, Wu CW, Lin VS. Mesoporous silica nanoparticles as controlled release drug delivery and gene transfection carriers. Adv Drug Deliv Rev 2008;60:1278–88.
[8] Canesi L, Ciacci C, Vallotto D, Gallo G, Marcomini A, Pojana G. In vitro effects of suspensions of selected nanoparticles (C_{60} fullerene, TiO_2, SiO_2) on Mytilus hemocytes. Aquat Toxicol 2010;96:151–8.
[9] Shukla A, Timblin CR, Hubbard AK, Bravman J, Mossman BT. Silica-induced activation of c-Jun-NH2-terminal amino kinases, protracted expression of the activator protein-1 proto-oncogene, fra-1, and S-phase alterations are mediated via oxidative stress. Cancer Res 2001;61:1791–5.
[10] Rangaswami H, Bulbule A, Kundu GC. Nuclear factor-inducing kinase plays a crucial role in osteopontin-induced MAPK/IkappaBalpha kinase-dependent nuclear factor kappaB-mediated promatrix metalloproteinase-9 activation. J Biol Chem 2004;279:38921–35.
[11] Chen F, Castranova V, Shi X, Demers LM. New insights into the role of nuclear factor-kappaB, a ubiquitous transcription factor in the initiation of diseases. Clin Chem 1999;45:7–17.
[12] Vallhov H, Gabrielsson S, Stromme M, Scheynius A, Garcia-Bennett AE. Mesoporous silica particles induce size dependent effects on human dendritic cells. Nano Lett 2007;7:3576–82.
[13] Bellocq NC, Pun SH, Jensen GS, Davis ME. Transferrin-containing, cyclodextrin polymer-based particles for tumor-targeted gene delivery. Bioconjug Chem 2003;14:1122–32.
[14] Larson DR, Zipfel WR, Williams RM, Clark SW, Bruchez MP, Wise FW, et al. Water-soluble quantum dots for multiphoton fluorescence imaging in vivo. Science 2003;300:1434–6.
[15] Bae Y, Lee S, Kim SH. Chrysin suppresses mast cell-mediated allergic inflammation: involvement of calcium, caspase-1 and nuclear factor-kappaB. Toxicol Appl Pharmacol 2011;254:56–64.
[16] Brown ME, Puleo DA. Protein binding to peptide-imprinted porous silica scaffolds. Chem Eng J 2008;137:97–101.
[17] Chung TH, Wu SH, Yao M, Lu CW, Lin YS, Hung Y, et al. The effect of surface charge on the uptake and biological function of mesoporous silica nanoparticles in 3T3-L1 cells and human mesenchymal stem cells. Biomaterials 2007;28:2959–66.
[18] Fadeel B, Garcia-Bennett AE. Better safe than sorry: understanding the toxicological properties of inorganic nanoparticles manufactured for biomedical applications. Adv Drug Deliv Rev 2010;62:362–74.
[19] Lu F, Wu SH, Hung Y, Mou CY. Size effect on cell uptake in well-suspended, uniform mesoporous silica nanoparticles. Small 2009;5:1408–13.
[20] Witasp E, Kupferschmidt N, Bengtsson L, Hultenby K, Smedman C, Paulie S, et al. Efficient internalization of mesoporous silica particles of different sizes by primary human macrophages without impairment of macrophage clearance of apoptotic or antibody-opsonized target cells. Toxicol Appl Pharmacol 2009;239:306–19.
[21] Kim SH, Lee S, Suk K, Bark H, Jun CD, Kim DK, et al. Discoidin domain receptor 1 mediates collagen-induced nitric oxide production in J774A.1 murine macrophages. Free Radic Biol Med 2007;42:343–52.
[22] Kim SH, Jun CD, Suk K, Choi BJ, Lim H, Park S, et al. Gallic acid inhibits histamine release and pro-inflammatory cytokine production in mast cells. Toxicol Sci 2006;91:123–31.
[23] Lee S, Suk K, Kim IK, Jang IS, Park JW, Johnson VJ, et al. Signaling pathways of bisphenol A-induced apoptosis in hippocampal neuronal cells: role of calcium-induced reactive oxygen species, mitogen-activated protein kinases, and nuclear factor-kappaB. J Neurosci Res 2008;86:2932–42.
[24] Kim SH, Sharma RP. Mercury-induced apoptosis and necrosis in murine macrophages: role of calcium-induced reactive oxygen species and p38 mitogen-activated protein kinase signaling. Toxicol Appl Pharmacol 2004;196:47–57.
[25] Kimber I, Hilton J, Dearman RJ, Gerberick GF, Ryan CA, Basketter DA, et al. An international evaluation of the murine local lymph node assay and comparison of modified procedures. Toxicology 1995;103:63–73.
[26] van den Berg FA, Baken KA, Vermeulen JP, Gremmer ER, van Steeg H, van Loveren H. Use of the local lymph node assay in assessment of immune function. Toxicology 2005;211:107–14.
[27] Carino IS, Pasqua L, Testa F, Aiello R, Puoci F, Iemma F, et al. Silica-based mesoporous materials as drug delivery system for methotrexate release. Drug Deliv 2007;14:491–5.
[28] Gu J, Fan W, Shimojima A, Okubo T. Organic-inorganic mesoporous nanocarriers integrated with biogenic ligands. Small 2007;3:1740–4.
[29] Lu J, Liong M, Zink JI, Tamanoi F. Mesoporous silica nanoparticles as a delivery system for hydrophobic anticancer drugs. Small 2007;3:1341–6.
[30] Yun HS, Park JW, Kim SH, Kim YJ, Jang JH. Effect of the pore structure of bioactive glass balls on biocompatibility in vitro and in vivo. Acta Biomater 2011;7:2651–60.
[31] Hudson SP, Padera RF, Langer R, Kohane DS. The biocompatibility of mesoporous silicates. Biomaterials 2008;29:4045–55.
[32] Napierska D, Thomassen LC, Lison D, Martens JA, Hoet PH. The nanosilica hazard: another variable entity. Part Fibre Toxicol 2010;7:39.
[33] Huang DM, Chung TH, Hung Y, Lu F, Wu SH, Mou CY, et al. Internalization of mesoporous silica nanoparticles induces transient but not sufficient osteogenic signals in human mesenchymal stem cells. Toxicol Appl Pharmacol 2008;231:208–15.
[34] Hamilton Jr RF, Thakur SA, Holian A. Silica binding and toxicity in alveolar macrophages. Free Radic Biol Med 2008;44:1246–58.
[35] Ghiazza M, Polimeni M, Fenoglio I, Gazzano E, Ghigo D, Fubini B. Does vitreous silica contradict the toxicity of the crystalline silica paradigm? Chem Res Toxicol 2010;23:620–9.
[36] Oberdorster G, Oberdorster E, Oberdorster J. Nanotoxicology: an emerging discipline evolving from studies of ultrafine particles. Environ Health Perspect 2005;113:823–39.

[37] Betti M, Ciacci C, Lorusso LC, Canonico B, Falcioni T, Gallo G, et al. Effects of tumour necrosis factor alpha (TNFalpha) on Mytilus haemocytes: role of stress-activated mitogen-activated protein kinases (MAPKs). Biol Cell 2006;98:233–44.
[38] Kang JL, Jung HJ, Lee K, Kim HR. Src tyrosine kinases mediate crystalline silica-induced NF-kappaB activation through tyrosine phosphorylation of IkappaB-alpha and p65 NF-kappaB in RAW 264.7 macrophages. Toxicol Sci 2006;90:470–7.
[39] Chang JS, Chang KL, Hwang DF, Kong ZL. In vitro cytotoxicitiy of silica nanoparticles at high concentrations strongly depends on the metabolic activity type of the cell line. Environ Sci Technol 2007;41:2064–8.
[40] Dobrovolskaia MA, Germolec DR, Weaver JL. Evaluation of nanoparticle immunotoxicity. Nat Nanotechnol 2009;4:411–4.
[41] Elias Z, Poirot O, Daniere MC, Terzetti F, Marande AM, Dzwigaj S, et al. Cytotoxic and transforming effects of silica particles with different surface properties in Syrian hamster embryo (SHE) cells. Toxicol in Vitro 2000;14:409–22.
[42] Murashov V, Harper M, Demchuk E. Impact of silanol surface density on the toxicity of silica aerosols measured by erythrocyte haemolysis. J Occup Environ Hyg 2006;3:718–23.
[43] Murdock RC, Braydich-Stolle L, Schrand AM, Schlager JJ, Hussain SM. Characterization of nanomaterial dispersion in solution prior to in vitro exposure using dynamic light scattering technique. Toxicol Sci 2008;101:239–53.
[44] Lin W, Huang YW, Zhou XD, Ma Y. In vitro toxicity of silica nanoparticles in human lung cancer cells. Toxicol Appl Pharmacol 2006;217:252–9.
[45] Ye Y, Liu J, Xu J, Sun L, Chen M, Lan M. Nano-SiO_2 induces apoptosis via activation of p53 and Bax mediated by oxidative stress in human hepatic cell line. Toxicol in Vitro 2010;24:751–8.